PROCEEDINGS B

rspb.royalsocietypublishing.org

Research

Cite this article: Van Houtan KS, Andrews AH, Jones TT, Murakawa SKK, Hagemann ME. 2016 Time in tortoiseshell: a bomb radiocarbon-validated chronology in sea turtle scutes. *Proc. R. Soc. B* **283**: 20152220. http://dx.doi.org/10.1098/rspb.2015.2220

Received: 15 September 2015
Accepted: 27 November 2015

Subject Areas:
ecology, environmental science

Keywords:
coral reefs, maturity, age determination, carbon-14, somatic growth, *Eretmochelys imbricata*

Author for correspondence:
Kyle S. Van Houtan
e-mail: kyle.vanhoutan@gmail.com

Electronic supplementary material is available at http://dx.doi.org/10.1098/rspb.2015.2220 or via http://rspb.royalsocietypublishing.org.

THE ROYAL SOCIETY PUBLISHING

Time in tortoiseshell: a bomb radiocarbon-validated chronology in sea turtle scutes

Kyle S. Van Houtan[1,2], Allen H. Andrews[1], T. Todd Jones[1], Shawn K. K. Murakawa[1] and Molly E. Hagemann[3]

[1]NOAA Fisheries, Pacific Islands Fisheries Science Center, 1845 Wasp Boulevard, Building 176, Honolulu, HI 96818, USA
[2]Nicholas School of the Environment, Duke University, 450 Research Drive, Durham, NC 27708, USA
[3]Vertebrate Zoology Collections, Bernice Pauahi Bishop Museum, 1525 Bernice Street, Honolulu, HI 96817, USA

Some of the most basic questions of sea turtle life history are also the most elusive. Many uncertainties surround lifespan, growth rates, maturity and spatial structure, yet these are critical factors in assessing population status. Here we examine the keratinized hard tissues of the hawksbill (*Eretmochelys imbricata*) carapace and use bomb radiocarbon dating to estimate growth and maturity. Scutes have an established dietary record, yet the large keratin deposits of hawksbills evoke a reliable chronology. We sectioned, polished and imaged posterior marginal scutes from 36 individual hawksbills representing all life stages, several Pacific populations and spanning eight decades. We counted the apparent growth lines, microsampled along growth contours and calibrated $\Delta^{14}C$ values to reference coral series. We fit von Bertalanffy growth function (VBGF) models to the results, producing a range of age estimates for each turtle. We find Hawaii hawksbills deposit eight growth lines annually (range 5–14), with model ensembles producing a somatic growth parameter (k) of 0.13 (range 0.1–0.2) and first breeding at 29 years (range 23–36). Recent bomb radiocarbon values also suggest declining trophic status. Together, our results may reflect long-term changes in the benthic community structure of Hawaii reefs, and possibly shed light on the critical population status for Hawaii hawksbills.

1. Introduction

The harvest of hawksbill sea turtles for the global tortoiseshell trade was enormous [1] with some estimates that 30 000 turtles were trafficked annually from 1950 to 1992 [2]. Few historical records exist for Hawaii, but recent analyses indicate the population was historically more abundant and geographically widespread [3]. Today, fewer than 20 females nest each year [4,5] suggesting that Hawaii hawksbills are the smallest sea turtle population on the Earth. Like other populations, Hawaii hawksbills inhabit coral reefs and estuaries [5,6], and forage on sponge, algae and macroinvertebrates [7]. However, much remains unknown about the basic life history of the population, which if understood, could aid long-term conservation and restoration efforts.

This situation is not uncommon for sea turtle populations worldwide [8]. Fundamental components of sea turtle life history—such as developmental biogeography, age and fecundity—require an immense monitoring effort and are difficult to estimate empirically. Often, these metrics are inferred from empirical proxies. Such methods may involve stable isotopes, skeletochronology, morphometrics, biotelemetry and modelling [5,9–13]. However, for their value to be understood, it is critically important that such proxies are independently calibrated and validated [13–15].

Bomb radiocarbon dating is widely used for age-validation in marine organisms. Environmental signatures of radiocarbon (^{14}C) shifted abruptly after the proliferation of thermonuclear testing in the mid-twentieth century [16]. The atmospheric diffusion of bomb ^{14}C generated distinctive regional

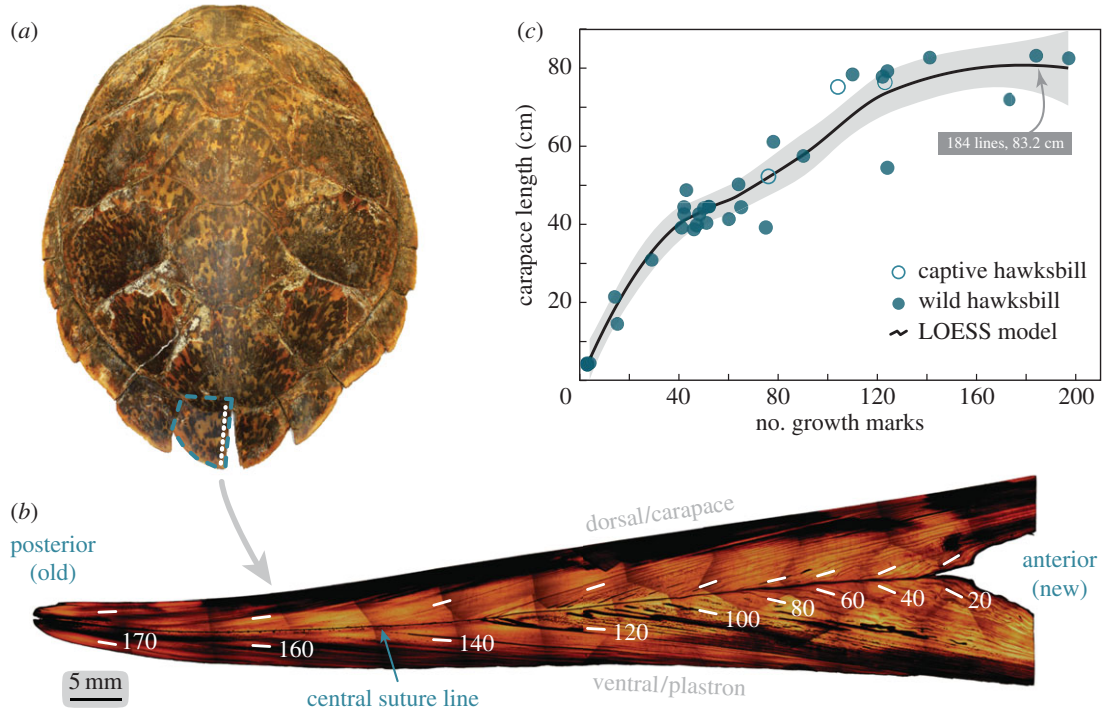

Figure 1. Interior structure of the posterior marginal scutes of hawksbill sea turtles contains an extensive chronology. (*a*) Adult female carapace measuring 83.2 cm straight length. Blue dashed outline is the PM scute, where the largest tissue record on the carapace resides. White-dashed line is the cross-section path. (*b*) Polished, composite image of the longitudinal cross-section of the PM scute identifying major features. Growth trajectory (old to new) runs left to right. The dark suture line that runs horizontally separates the dorsal/carapace and ventral/plastron portions of the shell. Parallel records occur on either side of this line. Shadows at individual image edges are peripheral halos from microscope field-of-view. Scute coloration varies naturally. (*c*) Growth line count for 36 hawksbills, obtained from the PM scute. A LOESS model fit through the data shows an expected growth curve form with three apparent stages (0–45 cm, 45–75 cm and greater than 75 cm) corresponding to known hawksbill stage classes. Shaded area is the 95% confidence band.

patterns of ^{14}C uptake in the upper ocean that are often described from hermatypic corals [17]. Such records provide a validated regional bomb ^{14}C series that are referenced to age long-lived fishes [18–20] and other taxa such as sponges and macroalgae [21,22]. Recent applications of bomb ^{14}C dating to fish otoliths (ear stones) in Hawaii [23] are an important precedent in applying this method to sea turtles. However, unlike fish otoliths, the carbon in sea turtle tissues is dietary, meaning an offset to the bomb ^{14}C reference can lead to a necessary adjustment for the age calibration, as was the case with porbeagle sharks [24]. Such trophic complications have been overcome in other sharks by establishing constraints to the bomb ^{14}C distribution and properly quantifying the limits of ^{14}C reference timeline [25,26].

Here we use bomb ^{14}C dating to understand the growth and maturity of hawksbill sea turtles in Hawaii. The successful application of bomb ^{14}C dating requires a cross section of samples from 1950 to present. In the Hawaiian archipelago, the particularly diagnostic bomb ^{14}C period occurred from 1955 to 1970 [23]. Immediately this presents logistical challenges as hawksbills are typically rare, and historical archives may be sparse or lack associated metadata. We therefore collaborated with a variety of institutional archives to amass sufficient specimens. We then built on previous studies [27,28] to develop procedures to describe the chronology in the keratinized scutes—the very tissues prized in the historical tortoiseshell trade. Next, we sampled multiple growth zones in individual turtles, quantified the radiocarbon in the samples and compared the results to regional coral reference records. We generated a range of age estimates for each turtle, and applied models to estimate somatic growth and maturity. The targeted result is the novel application of bomb ^{14}C dating and the first such validated maturity estimates for the population. We also discuss how our results may shed light on the population trajectory of Hawaii hawksbills.

2. Material and methods

(a) Carapace preparations

We collected hawksbill carapaces primarily through the strandings program of NOAA's Pacific Islands Fisheries Science Center (PIFSC), from the Bernice Pauahi Bishop Museum and the US Fish & Wildlife Service (Offices of Law Enforcement, Clark R. Bavin National Fish and Wildlife Forensic Laboratory, and National Wildlife Property Repository). Captive-reared carapaces were from the Hawaii Institute of Marine Biology and Sea Life Park Hawaii™. We collected and archived all specimens as specified under the US Endangered Species Act (USFWS permit TE-72088A-0). Originating institutions provided sample metadata.

All specimens (fresh and preserved shells) were prepared to separate the scutes from adjoining tissues. To achieve degradation naturally, we enclosed carapaces individually in perforated heavy-weight poly bags (ULINE™ recloseable 4 mil), and submerged in seawater for 2–7 days. Afterwards, we removed epibionts, cleaned scutes with soap and water, washed in 90% ethanol, air-dried in a fume hood and recorded morphometrics.

After examining many carapaces, and previous studies [27], we documented the largest keratin archive was in the ultimate posterior marginal scutes (PM). For each PM, we made 1.5 mm sagittal cross sections immediately lateral from the medial terminus (figure 1a,*b*), using a low-speed saw (Buehler Isomet™, No. 11-1280-170) with diamond wafering blades (Buehler 15HC, No. 11-4244). Owing to their irregular shape and size (figure 1a,*b*),

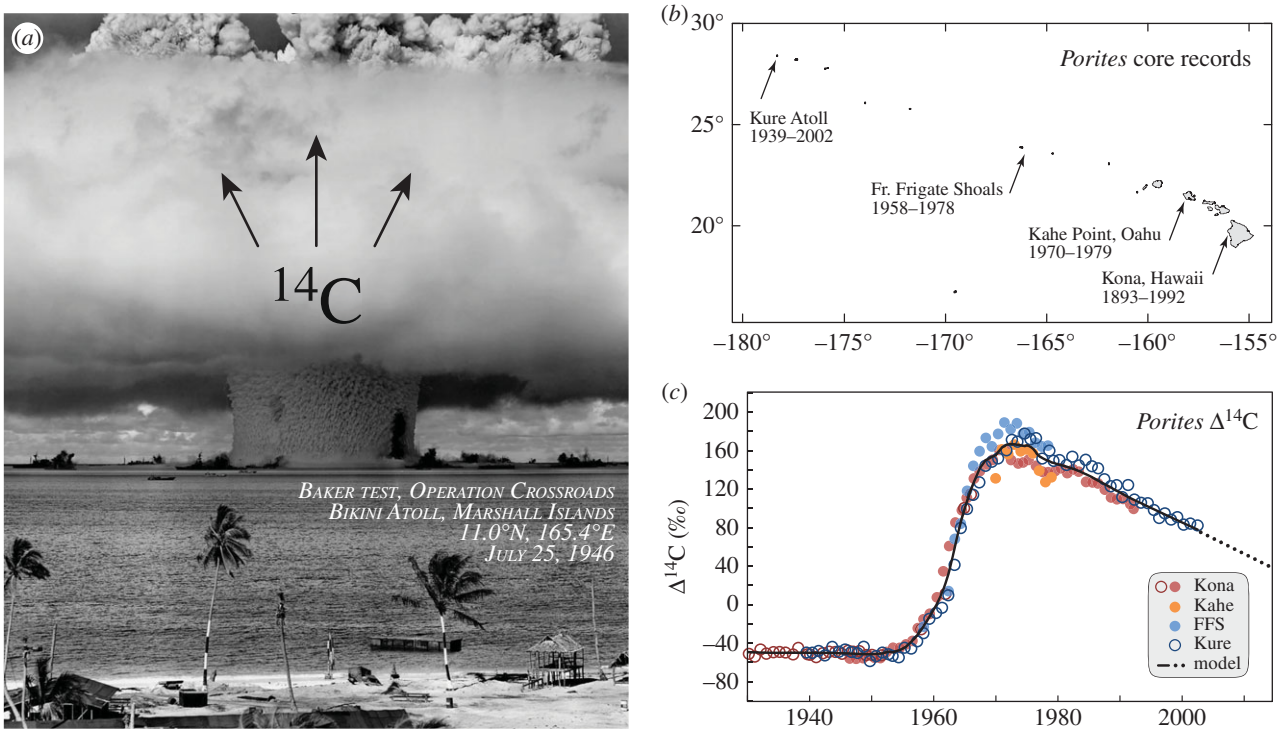

Figure 2. Hawaii coral cores provide a valid local bomb ^{14}C reference series. (*a*) The Baker nuclear detonation at Bikini lagoon in 1946, a 23 kt Mark III 'Fat Man' plutonium core bomb was one of the first in a series of tests that reached yields in megatons of TNT. The dark shape in the central water pillar is the silhouette from the battleship *USS Arkansas*. Later mid-twentieth century atmospheric nuclear detonations dispersed large amounts of ^{14}C across the biosphere, which accrued regionally at different rates and timelines. Image credit: US Government, public domain. (*b*) Sample sites in the Hawaiian archipelago providing *Porites* coral cores with date ranges. (*c*) Radiocarbon chronologies for *Porites* records. Black line is an ensemble model; dotted line is the linear extension through contemporary period.

we removed non-informing PM regions with a band saw (Ryobi®, No. BS904), thus allowing PMs to fit in the saw chuck clamps. We polished cross sections with a polishing wheel (Buehler ECOMET III™ 8″ Polisher) using silicon carbide lapping film (Mark V Laboratory®, A/O film 8″ NH) moving progressively from 30, 3 to 0.3 µm grit discs. The resulting sections represent the largest keratin chronology for each turtle.

(b) Microscopy and microsampling

We imaged the polished PMs with a standard microscope (scope: Olympus BX41™, camera: ImagingPlanet 20MPX™, adapter: Olympus U-TVO.5XC-3, firmware: IMT i-Solution Lite) at 1.25× magnification. This produced multiple (less than 70) images for each PM which we automated to a single mosaic using PhotoMerge® [29]. We identified the major anatomical landmarks, standardized mosaic orientation and counted growth lines (figure 1*b*). Moving from notch to tip, the lead author counted all apparent lines (dark β-keratin marks bounding α-keratin growth zones [28]), occurring along the central suture (figure 1*b*,*c*). By default, we restricted line transect counts to one side of the suture, but as parallel growth occurs along either side, we allowed this to vary if the transect path passed through melanized or other indistinct regions. In either case, we followed growth trajectory contours, from the anterior to posterior, to ensure all lines present were counted once.

We used a milling device (ESI New Wave Research, MicroMill™) equipped with a 0.5 mm spherical carbide bur bit (Brasseler USA, H71.11.005) to sample PM growth zones for 14 wild and three captive hawksbills from Hawaii (see electronic supplementary material). We mounted polished PM cross-sections onto glass slides using fine mesh double-stick tape. Similar to previous studies [23,25], we drilled a 1 × 10 mm linear path along growth line contours to 1 mm depth (just shy of specimen thickness). We repeatedly scanned the same paths at overlapping approximately 250 µm depths to obtain 1–3 mg of powder. We sampled the outermost and intermediary growth zones as feasible. (The oldest material was unavailable for two individuals.) We stored extracted material in pre-cleaned (at 550°C) aluminium foil pouches and sent samples to the National Ocean Sciences Accelerator Mass Spectrometry (NOSAMS) facility.

NOSAMS quantified bomb ^{14}C content via accelerator mass spectrometry (AMS). The AMS process combusted samples, generating CO_2, converted this to graphite and then quantified ^{14}C. NOSAMS reported ^{14}C as the fraction modern (Fm) from which we calculated $\Delta^{14}C$ using Stuiver & Polach's [30] correction for natural isotopic fractionation. Fm is the measured deviation of the $^{14}C/^{12}C$ ratio from a 'modern' sample. This reference is 95% of the radiocarbon concentration of the NBS oxalic acid I standard (SRM 4990B) normalized to $\delta^{13}C$ VPDB standard (−19‰) in the year 1950 [31]. Sample Fm values were corrected for isotopic fractionation using a $\delta^{13}C$ value either measured during AMS or as a measured value from a partitioned sample (robust and sample-specific $\delta^{13}C$ value). We corrected the final reported $\Delta^{14}C$ values to the estimated year of formation. The resulting data are the best estimate of how ^{14}C-depleted carbon sources from hawksbill diets may be reflected in the regional bomb ^{14}C signal.

(c) Radiocarbon reference records

In the Hawaiian archipelago (figure 2), radiocarbon records are available from massive *Porites* corals at shallow-depth locations from 1893 to 2002 ([32–34], AH Andrews 2016, unpublished data). These sites include Kure Atoll (28.392°N, 178.325°W); French Frigate Shoals (23.717°N, 166.100°W); Kahe Point, Oahu (21.30°N, 158.117°W) and Kona, Hawaii (19.517°N, 155.967°W) (figure 2*b*). From these records, we generated an ensemble radiocarbon series for Hawaii corals using a LOESS model [35]. We averaged sub-annual records to achieve a single annual $\Delta^{14}C$ value for each site to eliminate bias from

highly resolved series, representing the timeliest arrival of the bomb ^{14}C signal to Hawaii marine systems. We extrapolated the ensemble model from 2002 to present using a linear model from the LOESS values from 1985 to 2002 ($y = -3.20x + 6477.1$, $r = 0.999$). This provides a continuous, validated $\Delta^{14}C$ reference series for the Hawaiian archipelago from 1900 to 2012 that is highly resolved in the most diagnostic period (approx. 1955–1970).

When turtle collection dates are known, the newest scute material can be calibrated to the local coral $\Delta^{14}C$ reference series. This is important as hawksbills are omnivores [4,36] and their radiocarbon values will bear a trophic signature (a mix of timely and older ^{14}C sources). We, therefore, expect $\Delta^{14}C$ values from hawksbill scutes to be attenuated and perhaps phase-lagged by comparison with the coral series, similar to some sharks [24–26,37]. We built a radiocarbon time series for hawksbills from the date-referenced $\Delta^{14}C$ values for 14 Hawaii hawksbills collected from 1962 to 2012 (electronic supplementary material, table S2). We allowed the width, coral offset and coral lag of this curve to bear the canonical bomb $\Delta^{14}C$ form (e.g. Figure 2c) and chose those values that minimized the RMSE by comparison with validated observations. The resulting interval represents the possible dates of keratin deposition from Hawaii hawksbills, given its $\Delta^{14}C$ value.

(d) Age estimation and growth models

Having a calibrated radiocarbon series for Hawaii hawksbills, $\Delta^{14}C$ values from the oldest material can then be dated, and the turtle age estimated. However, a given $\Delta^{14}C$ value may occur over a range of dates [25,38], some of which may represent unrealistic growth. We therefore develop growth parameter bounds from the age-to-length relationship of the VBGF:

$$L_t = L_\infty(1 - e^{-k(t-t_0)}),$$

where t_0 represents the egg incubation period, L_∞ is the median straight carapace length (SCL) at first breeding [9,39]. The somatic growth parameter, k, is fit from the age–length data. For Hawaii hawksbills, $t_0 = -0.17$ (62.5 days) and $L_\infty = 81.0$ cm, both from empirical observations. L_∞ is the median SCL of 110 neophyte nesters from Hawaii and Maui (see electronic supplementary material, [4]). Age–length records from captive hawksbills are from PIFSC archives and published studies [40–44]. The VBGF relationship from captive hawksbill data sets the upper bound for k, and we fix the lower bound to 0.08 based on the literature [10,45–47].

We generated a minimum, mean and maximum age estimate for each turtle from the $\Delta^{14}C$ values and VBGF constraints. We used the above bounds for k to generate low and high estimates for birth year, and the calibrated $\Delta^{14}C$ interval to estimate minimum and maximum formation dates for the oldest scute material. The overlap of these two ranges sets the range for birth year, which when subtracted from the collection year, are the minimum and maximum age estimates. The average of these values is the estimated mean. When $L_t > L_\infty$ (3/12 turtles), the VBGF cannot be solved, and here we set $L_t = 80.9$ cm. For these turtles, the age estimates are constrained by the $\Delta^{14}C$ values, thus generating no bias.

We solved VBGF models for captive turtles with known ages, each age estimate scenario for wild samples, and estimated the age at maturity. To aid model fitting near the origin, we supplemented the 12 wild, microsampled specimens with one hatchling (4.3 cm SCL, 0.0 years) and one posthatchling (9.2 cm SCL, 4.2 months, 95% interval 1.7–6.6 months [5]). We fit models in RStudio [48] solving for k by minimizing the negative log-likelihood of model comparisons to the observed data (R code in the electronic supplementary material). We calculated the age at maturity, t_m, for each model from L_m, the length at maturity. Based on previous research [9], we assume $L_m = 0.975^*L_\infty$ and the complete 95% interval for t_m is the 0.95 and 0.99 values of L_∞ (77.0, 80.2 cm, respectively).

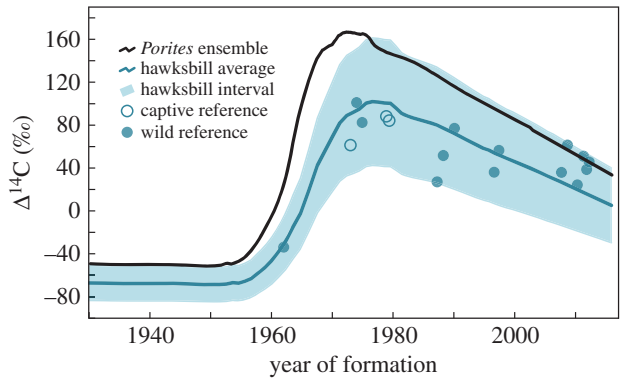

Figure 3. Calibrating the hawksbill $\Delta^{14}C$ curve from the coral record and validated hawksbill tissues. Owing to trophic effects, we expect the hawksbill $\Delta^{14}C$ curve to be attenuated and potentially phase-lagged compared to corals. Filled circles are ^{14}C values measured from the most recent keratin drill lines of 14 date-referenced Hawaii hawksbills, hollow circles are from three Hawaii captively reared hawksbills. Shaded area is the interval expected to account for all wild hawksbill observations.

3. Results

We obtained 36 complete hawksbill sea turtle carapaces from Hawaii (23), Indonesia (6), Marshall Islands (2), Tonga (2), Australia (1), with two of unknown origin. These turtles comprised five hatchlings (4–5 cm), three individuals from the cryptic early life-history stage (14–32 cm [5]), 19 juveniles (38–62 cm) and nine adults (72–84 cm). The recorded collection dates of these carapaces spanned 1962–2013. To document the general anatomy and growth line patterns in hawksbill PMs, figure 1 presents data from all populations. To control for potential variability between populations, we restricted the age estimates to the Hawaii samples (figures 3–5).

The number of growth lines in polished PM scute cross sections increased with carapace length, ranging from 3 to 197 (figure 1*c*). This relationship resembles published length-at-age relationships for sea turtles [9,11,15] with decreasing and eventually asymptotic growth. Model fits indicate three discrete stages at 0–45, 45–75, and greater than 75 cm (figure 1*c*), roughly equivalent to described hawksbill stage classes [4–6,45,47]. These patterns suggest that scute growth lines record a standard chronology throughout hawksbill ontogeny (electronic supplementary material, table S1 details all sample metadata).

Figure 2 describes the radiocarbon record in Hawaii *Porites* corals. The four collection sites (figure 2b) span 2400 km across the entire archipelago. Despite this distance, the radiocarbon values are relatively consistent (figure 2c), allowing a LOESS fit through the series to provide one continuous reference series for the Hawaiian Islands from 1900 to 2012. The resulting curve bears the expected [17] pre-bomb (1900–1955), bomb rise (1956–1971) and post-bomb decline (1972–present) pattern. Nonetheless, the steepness of the rise, the amplitude and location of the peak, and the rate of decline in $\Delta^{14}C$ values all require a regional description.

Date-referenced material from Hawaii hawksbill scutes has an attenuated $\Delta^{14}C$ signal compared with corals (figure 3). Radiocarbon values of dated material from 14 wild hawksbills were offset by an average of −42‰

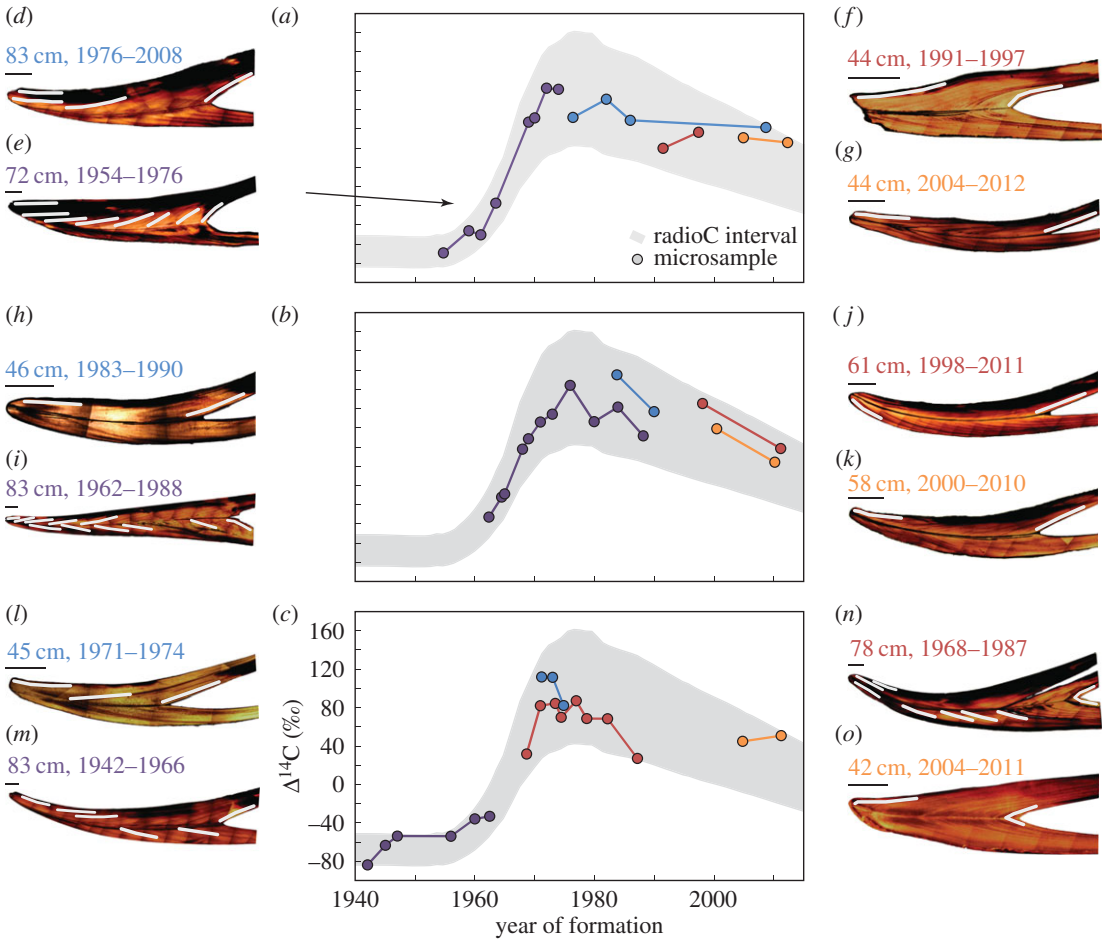

Figure 4. Bomb radiocarbon dating of hawksbill scute growth line sequences. (*a–c*) Microsampled drill lines from individual scute cross sections provide $\Delta^{14}C$ values throughout development, mapped onto the hawksbill $\Delta^{14}C$ curve. Newest tissue was date-referenced, oldest tissue dates are limited VBGF constrains and $\Delta^{14}C$ values, intermediary samples are interpolated. (*d–o*) Twelve cross-section images with sampled drill line transects. Measured lengths and lifespan dates are provided; scale bar for each inset represents 5 mm.

(min = 2‰, max = −98‰) relative to corals. This offset reflects their trophic status and cannot be tied to an age-related discrepancy because of the known collection dates. From the known-age hawksbill $\Delta^{14}C$ values, we generated a radiocarbon curve with confidence intervals (figure 3), which should capture the range of $\Delta^{14}C$ values for ontogenetic scute samples within older individuals. Other values through the ontogeny of each specimen remain attenuated (figure 4), providing evidence that age is not the primary factor in the observed offset from the timeliest coral records. It is in the region of the $\Delta^{14}C$ rise where constraints were the most diagnostic due to limits in the time of formation. From these values, we can assume that other measurements within and between individuals follow the trend established for determination of potential dates of formation. Using the hawksbill radiocarbon interval, figure 4 plots the chronologies from 12 Hawaii hawksbills with multiple growth zones sampled. Turtles have 2–11 microsampled zones paralleling growth line contours (figure 4*d–o*). Newest material is date-referenced, oldest material represents the mean age estimate (given the $\Delta^{14}C$ data and VBGF growth constraints) and intermediary zones were proportionally interpolated onto the expected $\Delta^{14}C$ values (figure 4*a–c*).

Figure 5 plots the length-at-age relationships for captive hawksbills and minimum, mean and maximum age estimates for wild turtles. Unsurprisingly, captive turtles grew fastest, reaching maturity in 12.3 years (range 10–15 years) with a k of 0.295 (figure 5*a*). We used this k value as a theoretical maximum, constraining minimum age estimates of wild Hawaii hawksbills. Figure 5*b* plots the minimum age scenario (fastest growth in wild hawksbills) showing turtles matured at 18.1 years (range 15–23 years) with $k = 0.201$. Under the mean growth scenario, turtles matured at 28.6 years (range 23–36 years) with $k = 0.128$ (figure 5*c*). For the maximum age scenario, turtles matured at 37.6 years (range 31–47 years) with $k = 0.098$ (figure 5*d*). Electronic supplementary material, tables S2–S3 provide full radiocarbon results and age estimates.

4. Discussion

This study uses a novel technique to assess growth and maturity of hawksbill sea turtles using carapace keratin. We present several results of interest. First, PM scutes record the chronology of growth in apparent lines, their number being proportional to turtle length (figure 1). Second, bomb $\Delta^{14}C$ values from date-referenced keratin samples reflect the trophic status of hawksbills, being attenuated relative to validated coral cores (figures 2–3). Third, constraints from growth and $\Delta^{14}C$ values provide age estimates for individual turtles (figure 4). VBGF models applied to various ageing scenarios yield estimates for age-at-maturity (figure 5).

Hawksbill sea turtles were uniquely exploited in the historical global tortoiseshell trade [1,2] because their

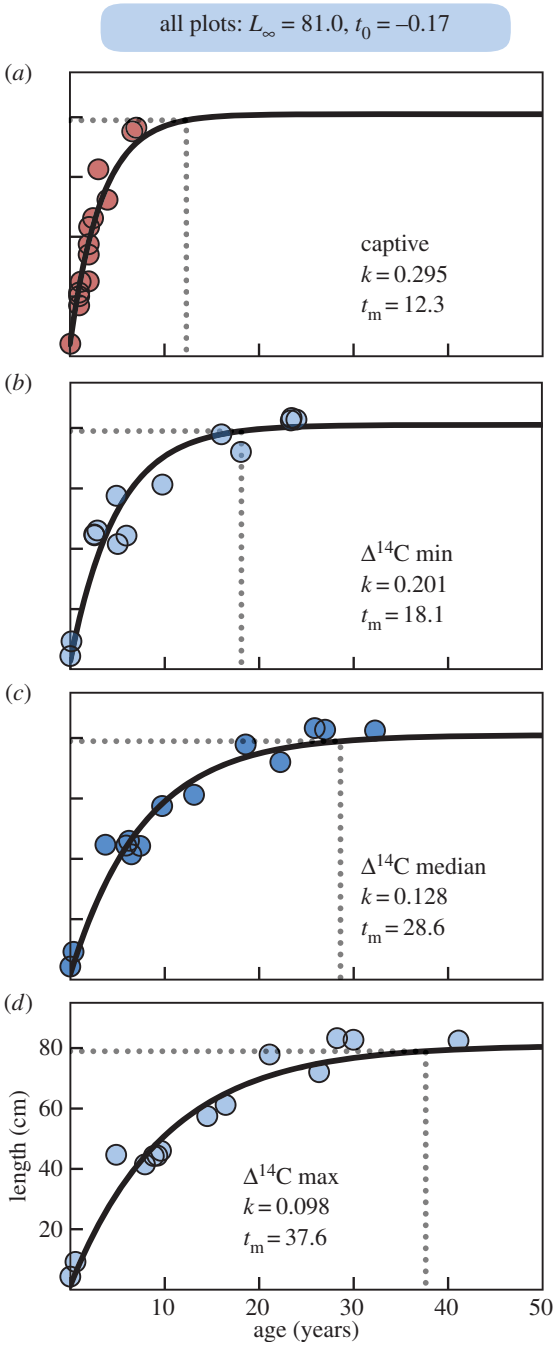

Figure 5. Growth model estimates for hawksbill age-at-maturity. (*a*) VBGF models fit to known ages of 16 captive-reared Pacific hawksbills places breeding maturity at 12.3 years (range 10–15 years), representing a potential ceiling of the somatic growth parameter, *k*, at 0.295. VBGF results considering (*b*) fastest, (*c*) mean and (*d*) slowest growth trajectories given the age range from the tissue Δ^{14}C values, and extreme values of *k*. All panels use listed values for asymptotic length, L_∞, and gestation time, t_0, obtained from empirical monitoring, but fit *k* to the age estimates. Together mean results from these models estimate *k* is 0.13 (range 0.10–0.20) and age at maturity is 29 years (range 18–38). From these results, hawksbills deposit eight scute growth lines annually (range 5–14).

carapaces contained abundant and structurally beautiful keratin (figure 1). But are scutes reliable for ageing? Otolith bones are widely used to age fishes, but are usually too small to construct a full time series within an individual [20,23]. Humeri bones are used to age sea turtles [11,46,49], but have an incomplete record as living tissue is reabsorbed. Vertebral and costal scute plates from hawksbill and other sea turtles [12,27,28,50] provide insights, but demonstrate significant abrasion and tissue loss. By contrast, PMs from hawksbills are large and may contain a near-complete chronology (figure 1*b*). Here, we selected PM scutes without significant external wear or damage, which was predominantly the case. Some polished PM sagittal cross sections viewed microscopically revealed minor damage (figure 4*f*) and ventral wearing (figure 4*d–m*). In these samples, growth zones from the dorsal section retained external layers. Although the methods we developed here may be suitable for ageing only hawksbills, the general tissue preparation and sampling procedures may be applied to other sea turtles and scute types.

The bomb ^{14}C dating method we employed indicates a mean maturity age for Hawaii hawksbills of 29 years (figure 5*c*). Recent analyses of Caribbean hawksbills suggest they can reach maturity much faster (10 years [45], though prior estimates were higher [51]). Owing to warmer ocean temperatures in the Caribbean [52], we might expect comparatively slower growth in Hawaii hawksbills, as occurs in similar comparisons for green turtles [15]. A recent analysis using skeletochronology estimated Hawaii hawksbills reach sexual maturity at 17–22 years [46], similar to our fast growth scenario (15–23 years). The authors of that study obtained all VBGF parameters ($t_0 = -1.44$ and $L_\infty = 95$ cm) from model fitting, however, where we derived values (see Material and methods). From empirical monitoring [4], measured nesting Hawaii hawksbills are always less than 90 cm and nest incubation averages 62.5 days. Following established methods [9,39], we derived VBGF parameters from these empirical data. Applying empirical derivations to VBGF parameters t_0 and L_∞ would likely change the skeletochronology-based maturity estimates, perhaps appreciably. Our results produced a theoretical ceiling for *k* from captive turtles (figure 5*a*, $k = 0.295$) as well as an observed minimum, mean and maximum estimate from wild Hawaii hawksbills ($0.1 < k < 0.2$, figure 5*b–d*).

Our estimate of hawksbill maturity is also higher than the recent estimate for green turtles (24 years [15]) which is unexpected. A recent effort estimated the VBGF $k = 0.173$ for Hawaiian green turtles [53]—within range but above the our mean value. Hawksbills are considered faster maturing than green or loggerhead sea turtles that may co-occur in neritic habitats [45,51]. As our results deviate from this pattern, it may suggest Hawaii ecosystems are currently unfavourable for hawksbills to thrive. To this end, historical data for Hawaii hawksbills, while limited, imply the population was significantly more abundant and widespread [3]. Dedicated monitoring further shows no significant population increases in Hawaii hawksbills from 1990 to present [4]. This is also unlike green turtles, whose nesting numbers have increased 5% annually as conservation efforts began in 1974 [54,55]. Although they occupy similar habitats, the trophic ecology of the two species may provide insights.

One potential explanation for the observed differences between green and hawksbill turtles in Hawaii is the observed coral reef decline [56,57]. Sponges, for example, are a preferred forage item for hawksbills [7,36] and in other regions their population status has been linked to reef health [58,59]. Shifts in the benthic reef community structure in Hawaii may therefore present unfavourable foraging conditions for hawksbills today. To this end, figure 3 indicates the Δ^{14}C values from date-referenced hawksbill tissues are more aligned with the coral values after the year 2000. Two

statistical tests that examine the probability of obtaining the observed runs of points above and below the model line formalize this observation. The number of runs (4) is on the low side of expectation for randomness (range 4–11, [60]), but a second test for run lengths [61] fails ($\chi_f^2 = 11.7$, $f = 5.5$, $p = 0.039$). This is evident as the samples from the last seven years are all above the ensemble line (figure 3). This pattern could result from isotopic fractionation [30], or it may reflect a trophic decline caused by a dietary shift from sponges to more timely carbon sources, like macroalgae. Preliminary stable isotope analyses support this idea. Comparing date-referenced tissues from four adult hawksbills in this study (two from 1987 to 1988 and two from 2007 to 2008), we find the δ^{15}N values declined on average from 15.7‰ (range: 15.6–15.8) to 8.8 (range: 8.4–9.1)—a drop of 7.0‰ in just two decades (KS Van Houtan 2016, unpublished data). Changes at the base of the food web can obscure stable isotope values, which subsequent compound specific stable isotope analyses of amino acid δ^{15}N may resolve [13]. Future analyses are required to make definitive claims regarding trophic status.

The physiology underlying keratin accretion and growth line deposition also deserves further attention. Integrating the line counts (figure 1*c*) with our age estimates from radiocarbon dating (figure 5*c*), suggests that mean deposition rates are eight lines per year (range 5–14). While variability between individuals and geographical location are likely factors, the processes that produce growth lines appear sub-annual, and perhaps monthly. Future studies may address relevant sub-annual physiological processes (such as climate e.g. [52]), and make comparisons to skeletal growth marks. From an evolutionary perspective, why hawksbills have the most massive carapace keratin deposits of all sea turtle species also deserves exploration.

Here we developed a novel technique to assess the development of hawksbill sea turtles. In doing so, we revealed a previously unrecognized clock within hawksbill carapaces (figures 1 and 4) and used bomb ^{14}C dating (figures 2 and 3) to calibrate its chronology. We encourage the application of these methods to hawksbill scutes from other ocean regions. Such studies may be especially aided by historical tortoiseshell specimens as such archives have great potential to address important ecological questions for sea turtle conservation. The approach we developed, using polished PM cross-sections avoids most of the stated pitfalls with tissue abrasion. Although we cannot guarantee perfect tissue retention in PMs from wild sea turtles, we expect any such influence to be negligible. Nonetheless, any effect to our results would be to increase the age that Hawaii hawksbills reach sexual maturity. This estimate (29 years, range 23–36 years) is unexpectedly high already. This delayed maturity may help interpret the lack of observed population recovery [4] and point to more fundamental challenges facing Hawaii coral reef ecosystems that could be hindering the population's long-term persistence.

Ethics. All research followed the NOAA Institutional Animal Care and Use Committee criteria.

Data accessibility. See the electronic supplementary material.

Authors' contributions. K.S.V., A.H.A. and T.T.J. designed the study; K.S.V. and A.H.A. performed the research; K.S.V. prepared the figures and drafted the manuscript. All authors contributed data, writing and reviewed the manuscript.

Competing interests. We have no competing interests.

Funding. A Presidential Early Career Award for Scientists and Engineers to K.S.V. supported this project.

Acknowledgments. G. Balazs, G. Phocas, A. Palermo, B. Baker, S. Green, A.-M. Lauritsen and D. Sprague provided specimens. J. Seminoff, A. Niccum, R. Dollar, S. Brunson, D. Francke and S. Handwork provided support. J. Davenport, E. DeMartini, D. Kobayashi and two anonymous reviewers improved earlier manuscript drafts.

References

1. Groombridge B, Luxmore R. 1989 *The green turtle and hawksbill* (*Reptilia: Cheloniidae*): *world status, exploitation and trade*, 601 p. Cambridge, UK: IUCN.
2. Donnelly M. 2008 Trade routes for tortoiseshell. SWOT report III, pp. 24–25.
3. Van Houtan KS, Kittinger JN, Lawrence AL, Yoshinaga C, Born VR, Fox A. 2012 Hawksbill sea turtles in the Northwestern Hawaiian Islands. *Chel. Conserv. Biol.* **11**, 117–121. (doi:10.2744/CCB-0984.1)
4. Seitz WA, Kagimoto KM, Luehrs B *et al.* 2012 Twenty years of conservation and research findings of the Hawai'i Island Hawksbill Turtle Recovery Project, 1989 to 2009. PCSU Technical Report, University of Hawaii, Honolulu, HI, 117 p.
5. Van Houtan KS, Francke D, Alessi S *et al.* Submitted. The developmental biogeography of hawksbill sea turtles in the North Pacific. *Ecol. Evol.*
6. Gaos AR *et al.* 2012 Shifting the life-history paradigm: discovery of novel habitat use by hawksbill turtles. *Biol. Lett.* **8**, 54–56. (doi:10.1098/rsbl.2011.0603)
7. Meylan AB. 1988 Spongivory in hawksbill turtles: a diet of glass. *Science* **239**, 393–395. (doi:10.1126/science.239.4838.393)
8. Carr A, Carr M, Meylan A. 1978 The ecology and migrations of sea turtles, 7. The west Caribbean green turtle colony. *Bull. Am. Mus. Nat. Hist.* **162**, 1–46.
9. Jones TT, Hastings MD, Bostrom, Pauly D, Jones DR. 2011 Growth of captive leatherback turtles, *Dermochelys coriacea*, with inferences on growth in the wild: implications for population decline and recovery. *J. Exp. Mar. Biol. Ecol.* **399**, 84–92. (doi:10.1016/j.jembe.2011.01.007)
10. Limpus CJ. 1992 The hawksbill turtle, *Eretmochelys imbricata*, in Queensland: population structure within a southern Great Barrier Reef feeding ground. *Wildl. Res.* **19**, 489–505. (doi:10.1071/WR9920489)
11. Zug GR, Balazs GH, Wetherall JA *et al.* 2002 Age and growth of Hawaiian green sea turtles (*Chelonia mydas*): an analysis based on skeletochronology. *Fish. Bull.* **100**, 117–127.
12. Reich KJ, Bjorndal KA, Bolten AB. 2007 The 'lost years' of green turtles: using stable isotopes to study cryptic lifestages. *Biol. Lett.* **3**, 712–714. (doi:10.1098/rsbl.2007.0394)
13. Seminoff JA, Benson SR, Arthur KE, Eguchi T, Dutton PH, Tapilatu RF, Popp BN. 2012 Stable isotope tracking of endangered sea turtles: validation with satellite telemetry and δ^{15}N analysis of amino acids. *PLoS ONE* **7**, e37403. (doi:10.1371/journal.pone.0037403)
14. Bjorndal KA, Bolten AB, Bennett RA, Jacobson ER, Wronski TJ, Valeski JJ, Eliazar PJ. 1998 Age and growth in sea turtles: limitations of skeletochronology for demographic studies. *Copeia* **1998**, 23–30. (doi:10.2307/1447698)
15. Van Houtan KS, Hargrove S, Balazs GH. 2014 Modeling sea turtle maturity age from partial life history records. *Pac. Sci.* **68**, 465–477. (doi:10.2984/68.4.2)
16. Broecker W, Peng T-H. 1982 *Tracers in the sea*, 690 p. Palisades, NY: Lamont-Doherty Earth Observatory.
17. Grottoli AG, Eakin CM. 2007 A review of modern coral δ^{18}O and Δ^{14}C proxy records. *Earth Sci. Rev.* **81**, 67–91. (doi:10.1016/j.earscirev.2006.10.001)
18. Andrews AH, Kalish JM, Newman SJ, Johnston JM. 2011 Bomb radiocarbon dating of three important reef-fish species using Indo-Pacific Δ^{14}C results. *Mar. Freshw. Res.* **62**, 1259–1269. (doi:10.1071/MF11080)
19. Baker Jr S, Wilson CA. 2001 Use of bomb radiocarbon to validate otolith section ages of red

snapper *Lutjanus campechanus* from the northern Gulf of Mexico. *Limnol. Oceanogr.* **46**, 1819–1824. (doi:10.4319/lo.2001.46.7.1819)

20. Kalish JM. 1993 Pre-and post-bomb radiocarbon in fish otoliths. *Earth Planet. Sci. Lett.* **114**, 549–554. (doi:10.1016/0012-821X(93)90082-K)
21. Darrenougue N, De Deckker P, Payri C, Eggins S, Fallon S. 2013 Growth and chronology of the rhodolith-forming, coralline red alga *Sporolithon durum*. *Mar. Ecol. Prog. Ser.* **474**, 105–119. (doi:10.3354/meps10085)
22. Fallon SJ, Guilderson TP. 2005 Extracting growth rates from the nonlaminated coralline sponge *Astrosclera willeyana* using bomb radiocarbon. *Limnol. Oceanogr. Methods* **3**, 455–461. (doi:10.4319/lom.2005.3.455)
23. Andrews AH, DeMartini EE, Brodziak J, Nichols RS, Humphreys RL, Marshall CT. 2012 A long-lived life history for a tropical, deepwater snapper (*Pristipomoides filamentosus*): bomb radiocarbon and lead–radium dating as extensions of daily increment analyses in otoliths. *Can. J. Fish. Aquat. Sci.* **69**, 1850–1869. (doi:10.1139/f2012-109)
24. Campana SE, Natanson LJ, Myklevoll S. 2002 Bomb dating and age determination of large pelagic sharks. *Can. J. Fish. Aquat. Sci.* **59**, 450–455. (doi:10.1139/f02-027)
25. Andrews AH, Natanson LJ, Kerr LA *et al.* 2011 Bomb radiocarbon and tag-recapture dating of sandbar shark (*Carcharhinus plumbeus*). *Fish. Bull.* **109**, 454–465.
26. Passerotti M, Andrews A, Carlson J, Wintner SP, Goldman KJ, Natanson LJ. 2014 Maximum age and missing time in the vertebrae of sand tiger shark (*Carcharias taurus*): validated lifespan from bomb radiocarbon dating in the western North Atlantic and southwestern Indian Oceans. *Mar. Freshw. Res.* **65**, 674–687. (doi:10.1071/MF13214)
27. Palaniappan PM. 2007 The carapacial scutes of hawksbill turtles (*Eretmochelys imbricata*): development, growth dynamics and utility as an age indicator. Thesis, Charles Darwin University, Australia.
28. Tucker A, Broderick D, Kampe L. 2001 Age estimation of *Eretmochelys imbricata* by sclerochronology of carapacial scutes. *Chel. Conserv. Biol.* **4**, 219–222.
29. Adobe. 2011 *Photoshop*. 12.1.1 × 32 ed. San Jose, CA: Adobe Systems Inc.
30. Stuiver M, Polach HA. 1977 Discussion: reporting of ^{14}C data. *Radiocarbon* **19**, 355–363.
31. Olsson IU. 1970 The use of oxalic acid as a standard. In *Proc. of the 12th Nobel Symposium on Radiocarbon Variations and Absolute Chronology* (ed. IU Olsson), p. 17. New York, NY: John Wiley & Sons.
32. Druffel ER. 1987 Bomb radiocarbon in the Pacific: annual and seasonal timescale variations. *J. Mar. Res.* **45**, 667–698. (doi:10.1357/002224087788326876)
33. Druffel ER, Griffin S, Guilderson T *et al.* 2001 Changes of subtropical North Pacific radiocarbon andcorrelation with climate variability. *Radiocarbon* **43**, 15–25.
34. Roark EB, Guilderson TP, Dunbar RB, Ingram BL. 2006 Radiocarbon-based ages and growth rates of Hawaiian deep-sea corals. *Mar. Ecol. Prog. Ser.* **327**, 1. (doi:10.3354/meps327001)
35. Cleveland WS, Devlin SJ. 1988 Locally weighted regression: an approach to regression analysis by local fitting. *J. Am. Stat. Assoc.* **83**, 596–610. (doi:10.1080/01621459.1988.10478639)
36. Graham SC. 2009 Analysis of the foraging ecology of hawksbill turtles (*Eretmochelys imbricata*) on Hawai'i Island: an investigation utilizing satellite tracking and stable isotopes. Thesis, University of Hawaii, Hilo.
37. Francis MP, Campana SE, Jones CM. 2007 Age under-estimation in New Zealand porbeagle sharks (*Lamna nasus*): is there an upper limit to ages that can be determined from shark vertebrae? *Mar. Freshw. Res.* **58**, 10–23. (doi:10.1071/MF06069)
38. Andrews AH, Kerr LA. 2015 Validated age estimates for large white sharks of the northeastern Pacific Ocean: altered perceptions of vertebral growth shed light on compliated Δ^{14}C results. *Environ. Biol. Fish.* **98**, 971–978. (doi:10.1007/s10641-014-0326-8)
39. Price ER, Wallace BP, Reina RD *et al.* 2004 Size, growth, and reproductive output of adult female leatherback turtles *Dermochelys coriacea*. *Endang. Species Res.* **5**, 1–8. (doi:10.3354/esr001041)
40. Witzell WN. 1980 Growth of captive hawksbill turtles, *Eretmochelys imbricata*, in Western Samoa. *Bull. Mar. Sci.* **30**, 909–912.
41. Bustard HR. 1979 Population dynamics of sea turtles. In *Turtles: perspectives and research* (eds M Harless, H. Morlock), pp. 523–540. New York, NY: Wiley & Sons.
42. Balazs GH, Nozoe M. 1978 *Preliminary report on the hawksbill turtle* (*Eretmochelys imbricata*) *in Indonesia, Philippines, Malaysia, and Singapore*. Honolulu, HI: Institute of Marine Biology.
43. Kajihara T, Uchida I. 1974 The ecology and fisheries of the hawksbill turtle, *Eretmochelys imbricata*, in southeast Asia. *Jpn. J. Herpetol.* **5**, 48–56.
44. Doi T, Marquez R, Kimoto H *et al.* 1992 *Diagnosis and conservation of the hawksbill turtle population in the Cuban Archipelago*. Tokyo, Japan: The Bekko Industry.
45. Hawkes LA, McGowan A, Broderick AC, Gore S, Wheatley D, White J, Witt MJ, Godley BJ. 2014 High rates of growth recorded for hawksbill sea turtles in Anegada, British Virgin Islands. *Ecol. Evol.* **4**, 1255–1266. (doi:10.1002/ece3.1018)
46. Snover ML, Balazs GH, Murakawa SK, Hargrove SK, Rice MR, Seitz WA. 2013 Age and growth rates of Hawaiian hawksbill turtles (*Eretmochelys imbricata*) using skeletochronology. *Mar. Biol.* **160**, 37–46. (doi:10.1007/s00227-012-2058-7)
47. van Dam RP, Diez CE. 1998 Caribbean hawksbill turtle morphometrics. *Bull. Mar. Sci.* **62**, 145–155.
48. RStudio-Team. 2014 *RStudio: integrated development for R* (*ver 0.98.1103*). Boston, MA: RStudio. (http://www.RStudio.com/ide)
49. Snover ML, Hohn AA, Goshe LR, Balazs GH. 2011 Validation of annual skeletal marks in green sea turtles *Chelonia mydas* using tetracycline labeling. *Aquat. Biol.* **12**, 197–204. (doi:10.3354/ab00337)
50. Vander Zanden HB, Bjorndal KA, Reich KJ, Bolten AB. 2010 Individual specialists in a generalist population: results from a long-term stable isotope series. *Biol. Lett.* **6**, 711–714. (doi:10.1098/rsbl.2010.0124)
51. Meylan AB, Donnelly M. 1999 Status justification for listing the hawksbill turtle (*Eretmochelys imbricata*) as critically endangered on the 1996 IUCN Red List of Threatened Animals. *Chel. Conserv. Biol.* **3**, 200–224.
52. Van Houtan KS, Halley JM, Marks W. 2015 Terrestrial basking sea turtles are responding to spatio-temporal sea surface temperature patterns. *Biol. Lett.* **11**, 20140744. (doi:10.1098/rsbl.2014.0744)
53. Van Houtan KS. 2015 Impacts of incidental bycatch from the American Samoa-based longline fishery to marine turtle populations, 25 p. PIFSC IR-15–027. NOAA Fisheries, Honolulu, HI, USA.
54. Seminoff JA, Balazs GH, Dutton PH *et al.* 2014 *Green turtle* (Chelonia mydas) *status review under the U. S. Endangered Species Act*, p. 592. Silver Spring, MD: NOAA National Marine Fisheries Service.
55. Kittinger JN, Van Houtan KS, McClenachan L, Lawrence AL. 2013 Using historical data to assess the biogeography of population recovery. *Ecography* **36**, 868–872. (doi:10.1111/j.1600-0587.2013.00245.x)
56. Bruno JF, Selig ER. 2007 Regional decline of coral cover in the Indo-Pacific: timing, extent, and subregional comparisons. *PLoS ONE* **2**, e711. (doi:10.1371/journal.pone.0000711)
57. Hunter CL, Evans CW. 1995 Coral reefs in Kaneohe Bay, Hawaii: two centuries of western influence and two decades of data. *Bull. Mar. Sci.* **57**, 501–515.
58. van Duyl FC, Moodley L, Nieuwland G, van Ijzerloo L, van Soest RWM, Houtekamer M, Meesters EH, Middelburg JJ. 2011 Coral cavity sponges depend on reef-derived food resources: stable isotope and fatty acid constraints. *Mar. Biol.* **158**, 1653–1666. (doi:10.1007/s00227-011-1681-z)
59. Wulff JL. 2006 Rapid diversity and abundance decline in a Caribbean coral reef sponge community. *Biol. Conserv.* **127**, 167–176. (doi:10.1016/j.biocon.2005.08.007)
60. Wald A, Wolfowitz J. 1940 On a test whether two samples are from the same population. *Ann. Math. Stat.* **11**, 147–162. (doi:10.1214/aoms/1177731909)
61. O'Brien PC, Dyck PJ. 1985 A runs test based on run lengths. *Biometrics* **41**, 237–244. (doi:10.2307/2530658)